Plant Cell Physiol. 45(7): 905–913 (2004)

The *ABNORMAL GAMETOPHYTES* (*AGM*) Gene Product of *Arabidopsis* Demonstrates a Role in Mitosis During Gamete Development

Anna-Marie Sorensen [1, 2, 3, 4], Sandra Kroeber [1] and Heinz Saedler [1]

[1] *Max Planck Institute for Plant Breeding Research, Department of Molecular Plant Genetics, Carl-von-Linné Weg 10, D-50829-Cologne, Germany*
[2] *Research School of Biological Sciences, Plant Cell Biology, Australian National University, Canberra, ACT, 0200, Australia*

Screening a T-DNA mutagenized population of *Arabidopsis thaliana* for reduced seed set and segregation distortion led to the isolation of the *abnormal gametophytes* (*agm*) mutant. Homozygous plants were never recovered, but heterozygous plants showed mitotic defects during gametogenesis resulting in approximately 50% abortion of both the male and female gametes. Isolation of the genomic sequence flanking the co-segregating T-DNA element led to the identification of a gene located on chromosome 5, predicted to encode a transmembrane protein. BLAST homology searches identified two homologous proteins that are not redundant, as is clear from the existence of the *agm* mutant. Unexpectedly, expression studies using the β-glucuronidase reporter gene suggest that *AGM* and its closest *Arabidopsis* homolog are mostly expressed in cells undergoing mitosis. Thus, *AGM* is not a gametophytic gene as originally speculated on the basis of segregation distortion, but rather classified as an essential gene crucial to the process of mitosis in plants.

Keywords: *Arabidopsis* — Gametogenesis — Semi-sterility — Mitosis.

Introduction

The generation of haploid gametes within the male and female structures of flowering plants, through meiosis, enables the alteration of the plant life cycle from its sporophytic to gametophytic generation. However, meiosis does not signal the end of gamete development, which further requires mitotic divisions on both the male and female side to achieve full differentiation. Gametogenesis has been well documented for plants such as *Arabidopsis thaliana*, *Nicotiana tabacum* and *B. napus* and both megaspore (Webb and Gunning 1994, Schneitz et al. 1995, Christensen et al. 1997, Christensen et al. 1998) and microspore (Scott et al. 1991, Goldberg et al. 1993, Twell et al. 1998) development can be divided into sporogenesis, spore development and gametogenesis, spore or gamete maturation. The establishment of polarity is essential in both male and female gametogenesis and both developmental pathways follow a consistent, sequential program that can be denoted by landmark events, useful to characterize mutants affected in these processes. Mutant screens depend on either altered genetic inheritance, such as that seen for the *prl* mutant, or seed abortion phenotypes have been utilized by a number of groups (Springer et al. 1995, Feldmann et al. 1997, Howden et al. 1998, Christensen et al. 1998, Grini et al. 2002, Sorensen et al. 2001) to isolate *Arabidopsis* gametophytic lesions.

A large number of *Arabidopsis* mutants affected in megagametogenesis have been isolated (Christensen et al. 1997, Christensen et al. 1998, Christensen et al. 2002, Drews et al. 1998, Feldmann et al. 1997, Grini et al. 2002, Springer et al. 1995, Moore et al. 1997). Some of these mutants such as *ada*, *tya* (Howden et al. 1998) *fem2*, *fem3*, *gfa4*, *gfa5* (Christensen et al. 1998), *gf* (Christensen et al. 1997) and *hadad* (Moore et al. 1997), affect mitotic division within the developing embryo sac which arrest at a 1-, 2- or 4-nuclei stage. Of these mutants, *fem3*, *gfa4*, *gfa5* and *gf* are classed as general gametophytic mutations, which mean the lesions affect development within both gamete types. The *fem3*, *gfa4*, *gfa5* and *gf* mutants arrest at the one-nucleate stage. One gamete development gene that has been cloned is *PROLIFERA* (*PRL*), which encodes a *MCM2-3-5*-like gene (Springer et al. 1995). In *prl* mutants, additional mitotic divisions are visualized within the embryo sac. *PRL1* is initially required during the G1 phase of cell division where the PRL protein becomes nuclear localized (Springer et al. 2000, Holding and Springer 2002). Homozygous mutants are lethal and heterozygous plants are semi-sterile showing only 50% transmission of the mutant allele through the female gametes. It is interesting to note that *PRL* expression is not limited to the female gametophyte, but has a more general role in dividing cells. While it is clear that specialized processes are at play during the mitotic events of spore development, some of the genes required for these processes are not specifically limited to expression in these cell types.

Following an interest to better understand the genetic regulation of megagametogenesis in *Arabidopsis*, with a future goal towards the artificial engineering of apomixis, or asexual reproduction in this obligate sexual species, we chose a large forward screening strategy to isolate mutants demonstrating a gametophytic inheritance. The idea being that this class of mutants would most likely reveal genes solely involved in gamete development. Here we report on the isolation in *Arabidop-*

[3] Present address: Research School of Biological Sciences, Plant Cell Biology, Australian National University, Canberra, ACT, 0200, Australia.
[4] Corresponding author: E-mail, sorensen@rsbs.anu.edu.au; Fax, +61-2-61254331.

sis of a novel gamete maturation mutant, *agm*, which was initially, but wrongly characterized as a general gametophytic mutant through forward screening for 50% abortion of the ovules and an altered segregation pattern of 1 : 1 wild type to mutant. However, as elucidated from *GUS* expression studies, the expression of *AGM* in sporophytic as well as gametophytic tissue, later allowed us to correctly classify the *AGM* gene as being lethal. We designated this locus as *ABNORMAL GAMETOPHYTES* (*AGM*) because heterozygous mutants show an approximate 50% abortion of both the pollen and ovules. Homozygous plants were not recovered and heterozygous plants are semi-sterile, showing a post-meiotic disruption of gamete formation during mitosis, arresting at the two-nucleate stage. This lesion is caused by a T-DNA insertion in, and partial deletion of, the putative promoter region of a gene located on chromosome 5 encoding for a protein predicted to contain six transmembrane domains.

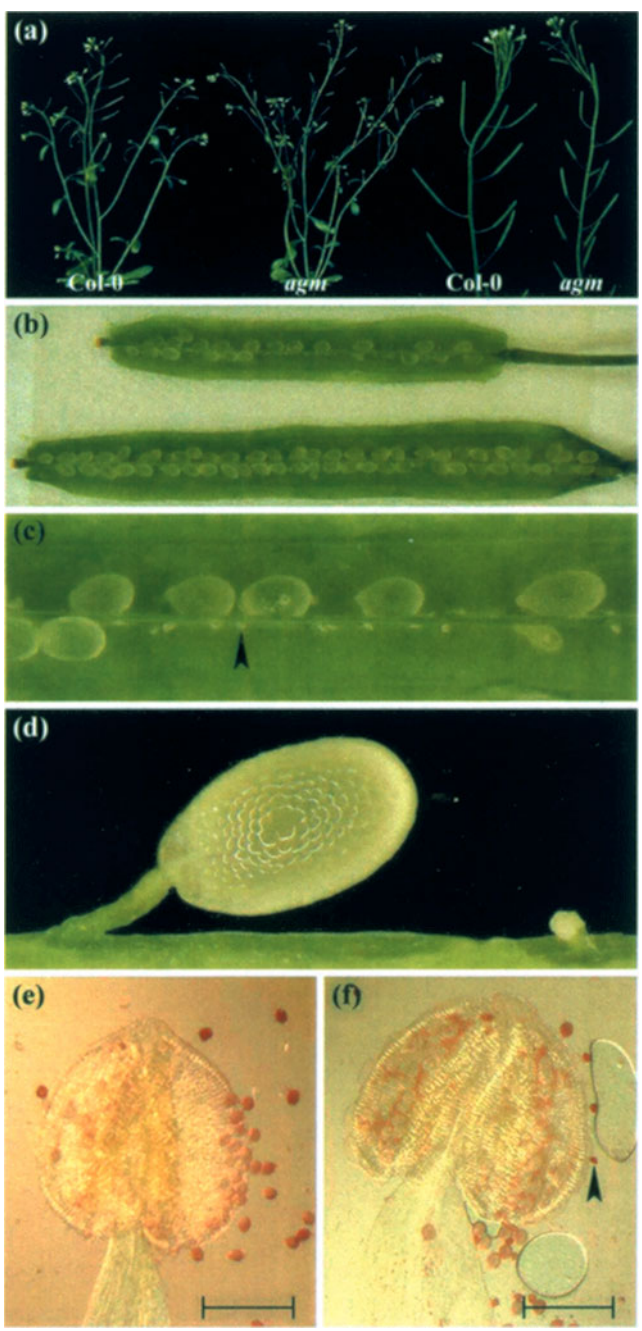

Results

Identification and gross phenotype of the agm mutant

The *agm* mutant was isolated from a forward screen for mutant plants having siliques containing approximately 50% aborted ovules. The *agm* mutant, belonging to an in-house T-DNA mutagenized population (Li et al. 2003), was chosen for further characterization on the basis that it showed a 1 : 1 segregation of heterozygous and wild-type plants in segregating families, typical for a mutation in a gametophytic gene. In an *agm* segregating population of 146 plants, 71 plants showed the mutant phenotype and 75 plants were wild type. As a result of the ovule abortion, *agm* heterozygous mutant plants are semi-sterile (Fig. 1a) and show a reduced silique length (Fig. 1b). On average, *agm* heterozygous siliques were 11.4 mm in length (SD = 0.78, n = 18) and wild-type siliques were 15.5 mm in length (SD = 0.86, n = 34), a significant difference (P <0.001) according to the statistical t test. On average mature *agm* heterozygous siliques show the presence of 21.2 (SD = 1.28, n = 22) wild-type ovules, which are fully viable and 18.6 (SD = 1.28, n = 22) aborted, undeveloped ovules (Fig. 1c, d); whereas wild-type siliques contained 55.8 wild-type ovules (SD = 1.51, n = 22) and 1.1 (SD = 0.74, n = 22) aborted ovules. Therefore on average *agm* mutant plants demonstrated 46.7% mutant ovules in comparison to 1.8% seen in wild type. In addition, examination of mature pollen from dehisced anthers of heterozygous *agm* flowers, indicates that approximately 50% of the pollen is also shriveled, having aborted normal development (Fig. 1f) following the completion of meiosis. On the basis of 50% pollen and ovule abortion *agm* was initially characterized as being a general gametophytic mutant line. However, since no

Fig. 1 (a–f) Phenotypes of wild-type (Col-0) and heterozygous *agm* mutant plants. (a) Gross phenotype of wild-type and *agm* mutant plant. Heterozygous *agm* mutant plant (left) resembles wild type (far left), except that the siliques are reduced in length, which is more evident on comparison of the wild-type (right) and *agm* mutant inflorescences (far right). (b) Comparison of a wild-type (Col-0, bottom) and heterozygous *agm* mutant silique (top). Wild-type siliques average 15.5 mm in length (SD = 0.86, n = 34), while siliques from *agm* mutants average 11.4 mm (SD = 0.78, n = 18). (c) Detail of a heterozygous *agm* mutant silique, showing the presence of 50% wild type and 50% smaller, aborted ovules (arrowhead). (d) High magnification detail of a wild-type (left) and aborted ovule present in an *agm* mutant silique. (e) Detail of a wild-type (Col-0) anther at dehiscence, showing the presence of homogeneous pollen. Scale bar = 200 μm. (f) Detail of a heterozygous *agm* anther at dehiscence, showing the presence of 50% shrunken, aborted pollen (arrowhead). Scale bar = 200 μm.

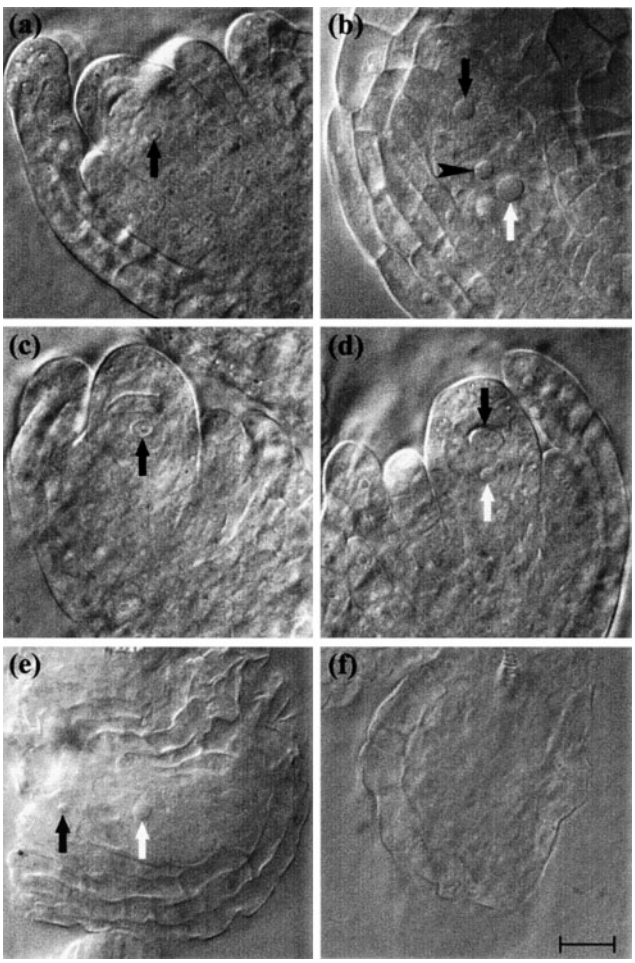

Fig. 2 (a–f) Cleared whole mounts of wild-type (Col-0) and heterozygous *agm* mutant ovules. (a) An ovule from an *agm* mutant plant showing the presence of a megaspore nucleus (arrow). (b) A mature wild-type ovule at stage FG7, showing the endosperm nucleus (white arrow), one of the two synergid nuclei (black arrow) and the egg cell nucleus (arrowhead). (c) An ovule from an *agm* mutant plant just prior to stage FG1 at the completion of meiosis, isolated from the same silique as that shown in (a), showing the most proximal surviving megaspore (arrow). (d) An *agm* mutant ovule at stage FG2, which unlike wild type has undergone an unequal first mitotic division, resulting in a larger more distal nucleus (black arrow) and a smaller proximal nucleus (white arrow). (e) An *agm* mutant ovule, showing the presence of two uneven nuclei (black and white arrows) separated by the formation of a cell wall. No other nuclei were visualized at other focal planes. (f) A degenerate *agm* mutant ovule devoid of nuclei or cell walls. Scale bar = 10 μm.

homozygous *agm* mutants were recovered and *AGM* expression was demonstrated in sporophytic as well as gametophytic tissue (see *GUS* expression studies below), *agm* was correctly classified as being a lethal gene. Aside from abnormal ovule and pollen development, the gross phenotype of heterozygous *agm* plants resembles wild type, indicating that the mutation is not dominant.

Inheritance of the agm mutation

Reciprocal crossing of heterozygous *agm* mutant plants to wild type, gave rise to heterozygous mutant progeny, whether the *agm* mutant was the pollen acceptor or donor (data not shown, due to statistically low numbers of seed recovered). This indicates that the *agm* mutation can be inherited through transmission in either the male or female gametophyte. However, in the absence of statistically valid data we can only estimate this to occur at a low frequency, considering a mutant/wild-type segregation ratio of 0.94 and the presence of 46.7% aborted ovules in heterozygous *agm* plants.

Gametogenesis is affected in agm mutants

The analysis of ovule development in *agm* mutants, using a chloral hydrate clearing protocol and normarski optics, indicates that megasporogenesis occurs Normally in *agm* mutants. In observations of *agm* ovules, meiosis always resulted in a single surviving megaspore (Fig. 2a). As occurs in wild-type development, the three most distal meiotic products degenerate, leaving only the most proximal megaspore surviving (Fig. 2c). Initial abnormalities in *agm* gametogenesis are only observed following the completion of meiosis and are described here using the denominated stages FG1 to FG7 as described by Christensen et al. (1998). In wild-type, the surviving megaspore (stage FG1) completes three rounds of mitosis to form an eight celled embryo sac (FG5), which then undergoes nuclear migration, cellularization and nuclear fusion of the polar nuclei to form the diploid endosperm (stage FG6) and finally antipodal cell death to give rise to mature embryo sac (FG7). At this stage of development (FG7), wild-type ovules are comprised of a large central cell with a diploid endosperm nucleus; two synergid cells and the egg cell. These latter three haploid cell types are present at the distal end of the ovule and their nuclei are typically located so that the synergid nuclei are most-distally located, while the egg cell nucleus sits at a proximal position within its cell (Fig. 2b). In *agm* mutant ovules, at stage FG2, the surviving megaspore attempts the first mitotic division; however, this event results in two unequally sized nuclei (Fig. 2d). As development proceeds, while half the ovules in heterozygous *agm* siliques are mature (FG7) and showing a wild-type size and phenotype, the remaining ovules are greatly reduced in size. Of an observed 81 smaller, abnormal ovules, 4.9% (four ovules) had attempted cytokinesis and cell walls were visible between the two nuclei were observed (Fig. 2e), while 7.4% (6 of 81) of these ovules showed the presence of the two unequal nuclei in an absence of cell wall formation. Only 1.2% (one ovule) showed the presence of three nuclei, perhaps indicative of an attempted second mitotic division while the remaining 86.4% appeared to have undergone tissue degeneration and were devoid of either nuclei or cell walls (Fig. 2f). Additionally, the size of the two abnormal nuclei resulting from the initial mitotic division varied between the mutant ovules, suggesting an unequal and inconsistent nuclear division.

Similarly to female development, microsporogenesis proceeds normally in *agm* mutants and abortion of approximately 50% of the pollen only occurs following meiosis and subsequent microspore release. Examination of buds 1.0 mm in length, predictive of the free microspore stage, showed the presence of homogeneous pollen within the anther locule (not shown). At this stage the microspore nuclei are still centrally located prior to pollen mitosis I. By a bud length of 1.1 mm, at a time when the microspore nuclei have migrated towards the pollen cell wall and undergone the first mitotic division, 50% of the pollen has aborted and collapsed (not shown). Thus at anther dehiscence, heterogeneous pollen is released from the mature anthers (Fig. 1f).

Isolation of the agm locus

Southern analysis using a T-DNA specific probe, of a small population of 12 plants segregating for the *agm* mutation, indicated these individuals contained 2–5 copies of the T-DNA in their genome (not shown). However, only one T-DNA insertion potentially co-segregated with the *agm* phenotype. Genomic DNA from a heterozygous *agm* individual carrying two T-DNA insertions, digested with Csp6I and linker PCR technology (see Materials and Methods), was utilized to isolate the corresponding genomic sequences flanking each 5′T-DNA end. The first 5′ T-DNA flanking sequence isolated, was shown by Southern analysis not to co-segregate with the *agm* phenotype, while the second 5′ flanking region did (data not shown). Subsequent BLAST search analysis, revealed 100% homology over 234 bp within the putative promoter region of At5g44860 (GenBank AC002342; BAC clone T19K24, contig K23L20.4), indicating the left border of the T-DNA had inserted at position 12304 (annotation according to the AC002342 GenBank entry). This gene is located on chromosome V and encodes a protein of unknown function. Subsequently, a gene-specific probe (see Materials and Methods), designed to detect the *Eco*RI RFLP generated by the T-DNA inserted into this gene confirmed that the insertion in At5g44860 co-segregated with the *agm* phenotype (Southern not shown). Typical of a gametophytic mutation, *agm* mutants were heterozygous for the T-DNA insertion into At5g44860, while phenotypically wild-type plants lacked any insertion and homozygous mutants were never recovered (either as indicated by Southern or PCR analysis). Interestingly, the *AGM* gene-specific probe showed the presence of a second hybridizing band, indicative of an *AGM* homolog (hereafter termed *AGM*-like) in the *Arabidopsis* genome, corroborated by computational analysis which also predicts a third family member (see *AGM* sequence analysis).

Isolation of the 5′ end of the T-DNA in At5g44860 indicated the 5′-end of the T-DNA was intact, but Southern blot hybridization, using the At5g44860 gene-specific probe, indicated that the T-DNA containing *Eco*RI RFLP fragment was somewhat truncated from a predicted 8.4 kb to around 7 kb, estimating a 1.4-kb deletion of the T-DNA. In order to obtain the 3′ integration site, a gel slice spanning the 7-kb marker, was eluted from an electrophoresis gel containing *Eco*RI-digested genomic DNA from an *agm* mutant. This DNA was eluted and inserted by shotgun cloning into pGEMTeasy. Subsequent electroporation into α-DH5 competent cells and colony hybridization, using the At5g44860 specific probe, allowed the recovery of the correct *Eco*RI genomic fragment. Sequence analysis subsequently revealed that the 3′-integration of the right border of the T-DNA had occurred at position 12453 (according to the GenBank entry annotation). As the ATG start site of At5g44860 is located at 12459, the ~4.5 kb T-DNA integration in *agm* is located 6 bp upstream of the ATG start site and results in an 148-bp deletion spanning the majority of the 5′UTR (see sequence analysis below) as well as 21 nucleotides of the putative promoter region. In addition, sequencing indicated that the entire 35S promoter region, normally contained at the right border T-DNA integration site was completely deleted, eliminating the possibility that the phenotype seen in *agm* could be due to an over-expression of the *AGM* gene.

AGM sequence analysis

A full-length Ceres cDNA clone (identification number: 31042) predicts a nucleotide length of 1,326 bp for the *AGM* gene (nucleotides 12325–13650 according to AC002342 GenBank entry). This cDNA contains a 5′ UTR (12325–12458) of 134 nucleotides and a 3′ UTR of 226 nucleotides (13425–13650), with the predicted coding region from 12459–13424, with no introns, thus encoding a protein of 321 amino acids in length. Computation BLASTP analysis shows the presence of two other *AGM* homologs in the *Arabidopsis* genome, namely At4g19950 and At1g31130, which show the highest available sequence homology to *AGM*. Like AGM, these homologs encode proteins of 321 amino acids in length. Over the entire coding region, At4g19950 shares 79% identity and 87% similarity to AGM, while At1g31130 shares 70% identity and 85% similarity. Interestingly, At4g19950 (*AGM*-like) was detected on a Southern blot, using the *AGM*-specific probe, while At1g31130 was not, presumably due to the reduction in homology at the nucleotide level over the probe specific sequence. All three of these homologs have no previously defined function. In addition, protein BLAST analysis indicates the presence of an *Oryza sativa* (japonica cultivar) homolog, BAB86411 of 329 amino acids in length, which shares a 44% identity and 58% similarity. Computational analysis (http://www.chembnet.org) predicts AGM to be a transmembrane protein containing six transmembrane domains at positions 32–52, 80–102, 163–187, 182–205, 220–239 and 255–275.

Complementation analysis

A 2,159-bp fragment surrounding the *AGM* locus was amplified by PCR and subcloned into a BASTA-resistant binary vector suitable to transform heterozygous *agm* mutant plants for complementation analysis (see Materials and Methods). This *AGM* region on chromosome V, utilized for

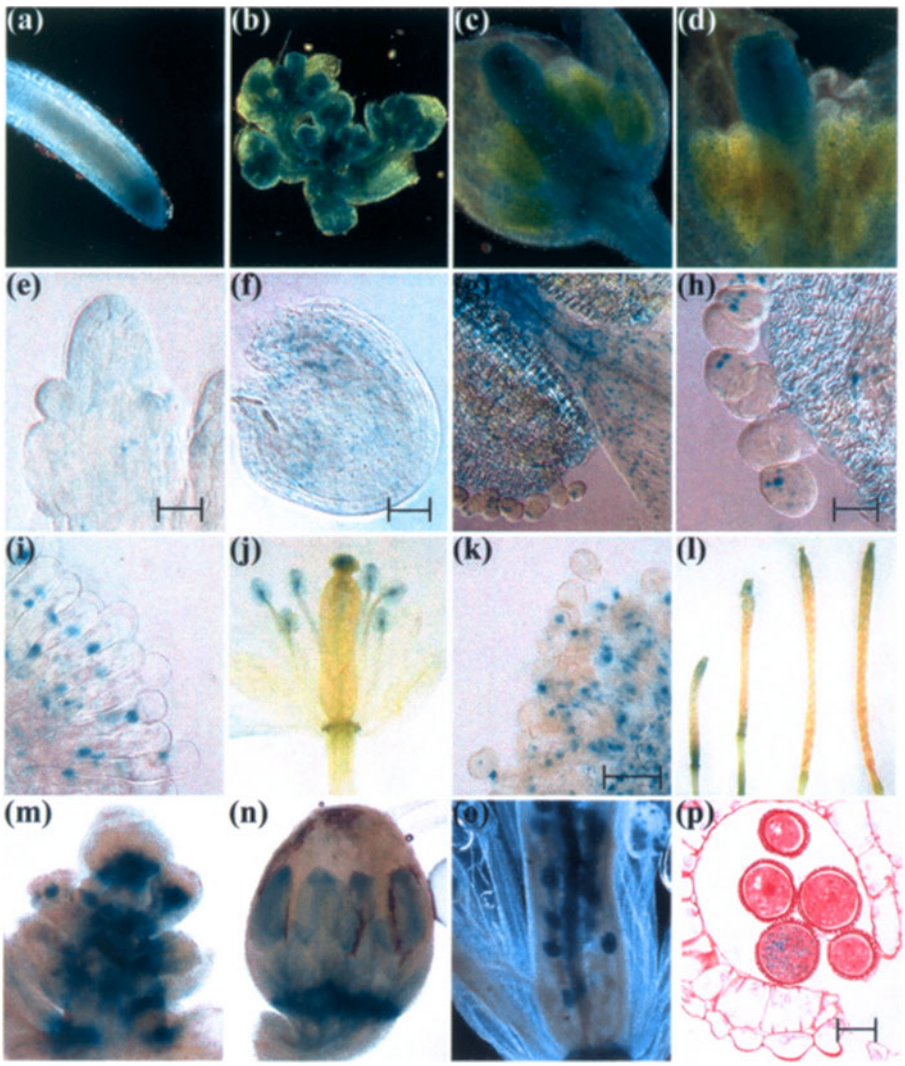

Fig. 3 (a–l) AGM promoter::*AGM*::*GUS*- and (m–p) AGM-like promoter::*GUS*-driven GUS expression patterns in a wild-type Col-0 background. Whole mount analysis of AGM promoter::*AGM*::*GUS* transgenic plants showing GUS localization in: the root meristem tip (a); floral buds of length 0.2 mm and less (b); a bud of 0.8 mm in length (c); a bud of 1.0 mm in length (d); early in ovule development at the stage prior to megaspore mother cell formation (e Scale bar = 10 μm); in an mature ovule at stage FG7 (f Scale bar = 20 μm); in a mature dehisced anther and pollen grains (h Scale bar = 20 μm); in mature stigmatic papillae prior to pollination (i); in the carpel and stamens of an open flower (j); in the outgrowing pollen tubes at pollination (k Scale bar = 50 μm) and in the most distal and proximal regions of developing siliques of lengths 5.8, 8.3, 12 and 13 mm respectively from left to right. Whole mount analysis of AGM-like promoter::*GUS* transgenic plants showing GUS activity in: buds of 0.2 mm or less. (m); a bud of 0.5 mm in length (n); ovules from an open flower (o); a transverse section of an anther taken from an open flower (p Scale bar = 20 μm).

complementation analysis was from nucleotide positions 11611 to 13770 (according to the GenBank AC002342 entry), encompassing 714 bp of putative promoter sequence as well as the 5′ UTR, coding region, 3′ UTR and an additional 120 bp downstream. T1 plants were selected using BASTA and grown to maturity. As BASTA resistance was transferred by both the mutating and complementing T-DNA insertion, PCR was utilized to identify individual plants transgenic for both the introduced wild-type copy of the *AGM* complementation construct as well as carrying the T-DNA insertion at the *agm* locus (see Materials and Methods). Five such individuals were identified and all these lines showed normal pollen and ovule development as well as seed set comparable to wild type. Two of these lines were analyzed by Southern analysis using an *agm*-specific probe (see Materials and Methods) and showed the presence of at least 7 and 9 copies of the transcript. Two of these transcripts are predicted to be the native *AGM* and *AGM*-like genes, thus indicating 5 and 7 copies of the complementing transgene present in these lines. Genetic segregation would estimate 1 in 64 and 1 in 256 mutant ovules in these plants respectively, if the transgenes are unlinked to the mutation. As these percentages are low in relation to the numbers of pollen in the anther and ovules present per silique, complemented lines were scored as wild type, phenotypically. Some plant lines showing the presence of the complementing and mutating T-DNA had a reduction from approximately 50% to approximately 25% aborted ovules (Southern analysis not performed), presumably due to a lower copy number of the complementing T-DNA element. Together, these data verify the mutating T-DNA within At5g44860 was responsible for the *agm* phenotype.

AGMprom::AGM::GUS and AGMprom-like::GUS expression studies

The expression patterns of the *AGM* (At5g44860) and *AGM*-like (At4g19950) genes were studied through fusions of the promoters with a reporter gene. The AGMpromoter::*AGM*::*GUS* (Fig. 3a–l) construct encompassed 714 bp of the AGM putative promoter region, followed by 134 bp of the *AGM*

5′UTR, the full *AGM* coding region minus the stop codon and a 3′ most translational fusion to the *uidA* gene. Whereas the AGM-like promoter::*GUS* construct contained a slightly more extensive putative promoter sequence extending 1 kb upstream of the ATG start site directly fused to *uidA* (Fig. 3m–p). Transgenic plants expressing either AGMprom::*AGM*::*GUS* or AGMprom-like::*GUS* constructs demonstrated similar patterns of GUS activity, mainly in regions of the plant undergoing rapid growth and cell division (Fig. 3), although not in developing seeds (Fig. 3l). GUS activity was never detected in the stems or mature leaves. GUS activity in the root tips of transgenic AGMprom::*AGM*::*GUS* plants (Fig. 3a) was indistinguishable from that seen in AGM-like prom::*GUS* lines (not shown), showing strong GUS activity at the meristematic region. Floral inflorescences (comprising the smallest closed buds up to a length of 0.2 mm, as well the floral meristematic region) showed strong GUS activity under the control of the AGM promoter with staining seen in all cell types, excluding the vascular system (Fig. 3b). AGM-like promoter counterparts (Fig. 3m), also showed GUS activity in the meristem; however, staining was spatially restricted to the lower half of emerging buds. As development continued, similar patterns of GUS activity in the floral buds under the control of either the AGM or AGM-like promoter were detected. In both promoters between bud lengths of 0.5 (Fig. 3n – AGM-like promoter) to 0.8 mm (Fig. 3c – AGM promoter), GUS activity was initially restricted to the abscission zone as well as to the peripheries of the anthers, but by 0.8 mm additional stronger GUS activity was visualized in the carpel, with lower, dispersed levels of GUS detected in all other floral tissues. By a bud length of 1.0 mm (Fig. 3d – AGM promoter), both promoters continued to show strongest activity in the carpels and abscission zone. This pattern of expression persisted under the control of either promoter up until a bud length of around 1.3 mm, after the event of mitosis within both gametes, as estimated from our studies to occur at around the 1.1 mm bud length stage. During mitosis, GUS activity was not limited to strong activity within the gametes, utilizing either promoter, but rather a low expression appeared to be evenly dispersed. This is reflected in the AGM promoter::*AGM*::*GUS* expression in the ovules show in Fig. 3e and f, from the initial appearance of the megaspore mother cell (Fig. 3e) until the formation of mature ovules (Fig. 3f). In larger floral buds, ranging in size from 1.5 to 2.0 mm, both promoters show similar expression patterns and GUS activity remains high in the abscission zone and at lower levels, which are evenly distributed throughout the floral tissue. By a bud length around 1.8 mm, only the top half of the carpel shows strong GUS activity. At the time of flower opening, GUS activity under the control of the AGM promoter is restricted to the stigmatic tissue and has additionally appeared within the anthers (Fig. 3j) and the vascular tissue of the anthers (Fig. 3g). Open flowers from a transgenic line expressing GUS under the control of the AGM promoter, showed strong GUS activity in the uppermost ovules and carpel vascular system (Fig. 3o). Examination of mature pollen (Fig. 3p – AGM-like promoter; Fig. 3h – AGM promoter) at dehiscence shows that GUS activity has become restricted to around 50% of the pollen grains and GUS activity appears as localized spots within the mature haploid male gametes. This localization appears to be nuclear as well as within other smaller scattered regions of the cytoplasm. At this time, mature ovules of AGM-promoter::*AGM*::*GUS* transgenic line showed a similar, but less dramatic localization of GUS (Fig 3f). The stigmatic tissue of these plants also shows localized GUS expression and each papilla appears to possess a single spot of activity (Fig. 3i). In addition, at pollen germination the GUS activity in AGMprom::*AGM*::*GUS* was seen to stain in localized but migrating regions of the outgrowing pollen tube (Fig. 3k). Regions of GUS activity were also restricted to the base and tips of developing siliques at all stages of silique elongation (Fig. 3l).

35S::AGM and 35S::AGM-like transgenic lines

The transformation of wild-type *Arabidopsis* with a 35S::*AGM* transgene gave rise to both fertile and semi-sterile T1 individuals as did transformation with the 35S::*AGM*-like construct (At4g19950 coding region). Over 100 lines were recovered for each of the 35S::*AGM* and 35S::*AGM*-like transgenes and approximately 10 and 12% of the lines were semi-sterile respectively. The semi-sterile lines from both 35S::*AGM* and 35S::*AGM*-like were phenocopies of heterozygous *agm* plants, showing the approximate 50% abortion of both the pollen and ovules (not shown). Attempts to utilize RT-PCR to detect the expression levels of *AGM* or the *AGM*-like coding region, in either wild-type or over expressing lines were unsuccessful, resulting in multiple PCR bands. Thus, the determination of transcript levels in these plants was not possible. However, as post-transcriptional gene silencing has been reported to cause variable levels of RNA down-regulation, it can only be speculated that the *agm* phenocopies recovered were at a threshold sufficient to allow sporophytic tissue development, but were insufficient to allow successful gametogenesis. Further genetic analysis of *AGM* expression levels are required to clarify this issue. However, the similarity of the phenotypes seen with either the *AGM* or *AGM*-like coding region may not be surprising, given the high similarity between the two coding sequences (see *AGM* sequence analysis above).

Discussion

The isolation of the genomic region flanking the T-DNA element responsible for the *agm* phenotype, led to the identification of At5g44860. This gene of previously unknown function, located on chromosome 5, was confirmed to be responsible for the *agm* mutation by successful complementation analysis. As complementation of heterozygous *agm* plants gave rise to wild-type plants directly in the T1 generation, the T-DNA transgene either integrated into the genome into mutant *agm* ovules before or during meiosis, or was targeted post-meiotically into

one of the few surviving mutant ovules shown to occur as indicated by partial transmission through the gametes. Southern and computational analysis indicated that this protein belongs to a small protein family in *Arabidopsis*, comprising two other family members At4g19950 and At1g31130, which are located on chromosome 4 and 1 respectively. These proteins, all of 321 amino acids in length, contain motifs indicative of a transmembrane protein family, with At4g19950 and At1g31130 sharing respectively 79% and 70% identity to At5g44860.

The *agm* mutation shows a lethal inheritance and causes mitotic defects in approximately 50% of both the mega and microgametophyte of heterozygous plants. Homozygous plants were not recovered. Meiosis proceeds normally in *agm*; however, subsequent mitosis events are disrupted in mutant mega and microgametes. Partial *agm* transmission through the gametes allows the mutation to be recovered in the next generation. During ovule development in heterozygous *agm* siliques, abnormalities were initially visualized following attempts at the first mitotic division in megagametogenesis. Only this first of the three usual rounds of mitosis was usually initiated, ultimately giving rise to approximately 50% small, undeveloped ovules. While the majority of abnormal ovules were arrested at the 2-nuclei stage, once in 81 observed cases, a presumed attempt at a second mitotic division was visualized.

On the male side, pollen meiosis also appeared normal and *agm* microgametogensis only arrests subsequently following microspore release, at a time when the pollen are undergoing their first mitosis. Thus *AGM* is required post-meiotically for important cellular process during reproductive development in both gamete types. Interestingly, cytokinesis was visualized in some of the mutant *agm* ovules, even though mitotic events were not completed. This may suggest that the *AGM* gene pathway does not signal the subsequent events of phragmoplast and cell wall formation, but rather these events are under an alternate or parallel genetic pathway.

It is interesting to note that while heterozygous *agm* mutant plants do not have an affect per se on the overall gross morphology of plants (i.e. the heterozygous condition of *AGM* appears to fulfill its role in sporophytic tissue) is does seem apparent that the presence of the *agm* mutation results in a reduction in overall ovule number in *agm* in comparison to wild type. One explanation may be that the reduction is silique elongation that occurs in *agm* mutants (as the presence of smaller aborted ovules require less space) may directly or indirectly feedback to cause a reduction in ovule primordia initiation.

AGM expression patterns

Sequence analysis shows that *AGM* is part of a three-gene family. Although RT-PCR was unable to differentiate between the gene family members, promoter GUS analysis was undertaken utilizing the 5′ regions, upstream of the ATG of both At5g44860 and At4g19950. Progeny containing either the AGM promoter::*AGM*::*GUS* or AGM-like promoter::*GUS* transgene showed similar patterns of expression, with GUS activity detected in both sporophytic and gametophytic cells. Thus GUS activity was not solely restricted in the case of either promoter, to the cells involved in gametogenesis. Indeed, the levels of GUS activity were present at much lower levels in gametophytic than sporophytic tissue. However, the lower levels visualized in the developing gametes may not be indicative of the importance of the *AGM* family in the process in which they are involved, but rather may just be a reflection of the mass of cells and cytoplasm being viewed. While the GUS data indicate that the *AGM* and *AGM*-like genes are expressed during vegetative cell development, the absolute requirement for *AGM* in gametogenesis is underlined by the fact that complementation is possible in the heterozygous plants and that mutants show an effect at the haploid level. However, the extensive expression of *AGM* is consistent with a possible broad role in several aspects of development, rather than as a general gametophytic gene. Thus the use of altered segregation patterns to identify mutations specific to the gametophyte, has its limitations in that other genes critical to cell development will also be identified, but as they can only be transmitted in a heterozygous form they give the impression of being gametophyte specific.

As a generalization indicated by GUS expression patterns, both the *AGM* and *AGM*-like promoter appear to change their spatial expression pattern during bud and floral development and these patterns appear to reflect growth and development. Extrapolating from the mitotic defects seen in the *agm* gametes as well as the strong GUS activity seen in the root tip, it appears that the GUS activity demonstrated in the sporophytic tissue is a reflection of mitotic activity or of the growth that usually precedes cell division. At a later stage of pollen development during dehiscence, *GUS* fusions result in GUS activity clearly localized to small regions, evenly distributed throughout the mature pollen, as well as appearing to stain the nuclei. However, contrary to active mitotic localization, GUS activity was visualized during pollen tube germination and this GUS localization migrated with pollen tube extension. GUS activity was also visualized within in mature stigmatic papillae. Additionally, post-fertilization GUS activity was absent in developing ovules, while the respective siliques retained GUS activity at their extremities. Taking the GUS data together with the abnormal nuclear division in *agm* gametes and the transmembrane motifs present in this gene family it is tempting to speculate a role for the *AGM* family in nuclear separation or migration mediated via the *AGM* family acting as a form of membrane anchor protein. However, a more detailed analysis of gene expression or protein localization is required to determine the role of the AGM proteins. Unfortunately, of a total of over 100 *AGM*::*GFP* and *AGM*-like promoter::*GFP* transgenic plants generated, in an attempt to clarify the GUS data obtained, no GFP florescence was detected.

Interestingly but perhaps not surprising, considering the high similarity between the coding regions, both 35SCaMV::

AGM and 35ScaMV::*AGM*-like over expressing transgenic lines gave rise to fertile and semi-sterile individuals. These semi-sterile lines, utilizing either coding sequence, like *agm* showed heterogeneous pollen and ovule abortion. In the absence of RT-PCR, it can only be suggested that these *agm* phenocopies arose due to co-suppression of *AGM* as has been reported for other cases (Sorensen et al. 2003). However, co-suppression in this case would rely on a partial down-regulation of the *AGM* transcript, to explain why a phenotype is only visualized in the gametophytic and not sporophytic tissue. Based on the lethality of *agm* it would be consistent that only partially down-regulated plants would be recovered. However, in the absence of expression data to support a co-suppression theory, this observation remains speculative. While the At4g19950, *AGM*-like gene is expressed in the floral tissue and gametes, it is not able to substitute for the role of *AGM* in gamete mitosis and thus while these proteins may share similar functions they are not redundant, as is clear from the existence of the *agm* mutant. In this respect, complementation of the *agm* heterozygous line with the *AGM-like* gene(s) might be more revealing.

Materials and Methods

Mutant populations and growth conditions

The *agm* mutant was isolated by screening a collection of in-house *A. thaliana* T-DNA mutagenized lines (Li et al. 2003). The Col-0 ecotype used to generate the population was transformed by *Agrobacterium*-mediated floral dipping to introduce random, approximately 5.8-kb T-DNA integrations into the genome. The binary transformation vector used, pAC106, contains the SUL1 ORF for resistance against the herbicide sulfadiazine (4-amino-*N*-2-pyrimidinylbenzenesulfonamide, Sigma-Aldrich, Germany). Vector pAC106 (AJ537513) contains two full-length 35S CaMV-promoters. One is located at the T-DNA right border, while the second promotes resistance against the herbicide sulfadiazine.

Nucleic acid analysis

DNA isolation was carried out as previously described (Sorensen et al. 2003). PCR generated probes. A 476-bp PCR-generated T-DNA probe for Southern analysis was generated using the following primers 378.fp (anneals in pAC106 at nucleotide positions 378–404: 5′-TATCCACAGAATCAGGGGATAACGCAG-3′) and 854.rp (anneals in pAC106 at 854–828: 5′-ACCTCGCTCTGCTAATCCTGTTACCAG-3′), using the pAC106 T-DNA binary vector as a template. An At5g44860 gene-specific probe was generated using primers B617.B.2.fp (anneals at positions 12634–12660 in AC002342: 5′-AGCTAGATGCAACTCCTCCTTCAGATC-3′) and B617.B.2.rp (anneals at positions 13397–13371 in AC002342: 5′-ACTGCTCTTTAACGGCACATAGTCACC-3′). Probes were generated by PCR using the 3 step PCR cycling conditions for 40 cycles: 94°C, 40 s; 65°C, 1 min; 72°C, 2 min.

T-DNA flanking sequence isolation was carried out based on the method of Steiner-Lange et al. (2001). Genomic DNA from a heterozygous *agm* individual was digested with Csp6I and ligated with the linker APL1632. A linear PCR to amplify the 5′-flanking region was carried out using a T-DNA annealing primer 9750as (5′-ATAATAACGCTGCGGACATCTACATTTT-3′) followed by a second PCR using a nested T-DNA primer 9697as, (5′-CTCTTTCTTTTTCTCCATATTGACCAT-3′) and LR26. The resulting PCR product was ligated into pGEMTeasy (PROMEGA) and electroporated into α-DH5 competent cells. Minipreparations of DNA were sequenced using the M13 forward sequencing primer.

Complementation of the agm mutant

PCR using the EXPAND long template PCR system (ROCHE) was carried out on the *AGM* containing IGF_B122K2419 BAC clone, created by Tereza Mozo and obtained from the RZPD resource center (https://www.rzpd.de). BAC clone DNA was extracted using the Nucleobond PC 500 kit (MACHEREY-NAGEL). A total of 125 ng of DNA was used in 30 PCR cycles (94°C, 10 s; 63°C, 30 s; 68°C, 2 min) using the 10× buffer 2, set up according to manufacturer's instructions using a 5′ primer, 48.617.3.fp (XhoI:11611–11637, 5′-AACCTCGAGCGATATGAACTTCTTCTTCGTCGTGAG-3′) and a 3′ 48.617.3.rp (HindIII:13770–13744, 5′-ACCAAGCTTCATGTAACCCACAATGCTTGAATCTCC-3′). All primer annealing positions within the BAC clone refer to numbers annotated on the BAC clone entry of the ENTREZ database (AC002342). The ~2 kb PCR product was ligated into pGEMTeasy, creating p617–11 and sequenced. Sequencing showed 2 bp errors, both in the promoter region at positions 11776 (A to G transition) and a second A to G transition at position 12044. The *AGM* promoter-gene was excised from p617–11 as an *Xho*I, *Hin*dIII fragment and sub-cloned into an *Xho*I, *Hin*dIII-digested pBHS binary vector creating p617–26. The pBHS binary vector is based on the pGPTV-BAR binary vector (as previously described by Sorensen et al. 2003) with the *Hin*dIII/*Sac*I fragment being replaced with a *Hin*dIII/*Sac*I polylinker (polylinker: *Hin*dIII, *Xba*I, *Bsi*WI, *Xho*I, *Sca*I, *Sma*I, *Sac*I). Electroporation was used to introduce p617–26 into the *Agrobacterium* strain GV3101 and floral dipping was used to transform mutant plants heterozygous for the *agm* mutation.

PCR primers used to confirm the presence of the complementing *AGM* coding region were B617B2.fp (12634–12660, 5′-AGCTAGATGCAACTCCTCCTTCAGATC-3′) and pNOS32 (5′-GATCTTGATCCCCTGCGCCATCAGA-3′, located within the pNOS promoter of pBHS binary vector), while primers to test for the presence of the mutating T-DNA were B617B.fp (12096–12125, 5′-GAATAGTACCGAATTCCTACAATGCTTACG-3′) and 9697as (5′-AATTGGTAATTACTCTTTCTTTTTCTCCATATTGA-3′, located within the AC106 integrating T-DNA).

Ovule clearing

Siliques and ovules were fixed overnight using 9 : 1 acetic acid : ethanol and then washed with 90%, then 70% ethanol before clearing in 8 : 1 : 2 chloral hydrate : glycerol : water.

Promoter GUS fusions

A 848 bp 5′ upstream region of the *AGM* coding region was PCR amplified (EXPAND, buffer 2, ROCHE; 30 PCR cycles of 94°C, 10 s; 61°C, 30 s; 68°C, 1 min) from the IGF_B122K2419 clone using primers 48.617.3.fp (XhoI:11611–11637, 5′-AACCTCGAGCGATATGAACTTCTTCTTCGTCGTGAG-3′) and 48.617.fr.rp (12471–12447, 5′-CAGCGAGATCCATGGCTGAGATTAG-3′). The PCR product was ligated into pGEMTeasy, creating p617–12 and sequenced. Sequencing showed two errors, 1 bp change of an A to a G at position and the deletion of an A at 11666. The AGM promoter was excised from p617–12 as an *Xho*I-blunt, *Nco*I fragment and ligated upstream of the *uidA* gene, by insertion into *Sma*I, *Nco*I-digested pblu-KS35SGUS vector to create p617–35 (replacing the CamV35S promoter with the AGM promoter). The pblu-KS35SGUS plasmid is based on the pBluescript KS vector (STRATAGENE), containing the full-length 35S cauliflower mosaic virus promoter upstream of the gene. p617–35 was digested with *Nco*I and a *Nco*I *AGM*-coding region, PCR generated to remove the TAA stop codon [generated utilizing the EXPAND kit and

AGM BAC clone as described above in conjunction with PCR primers 617.ncoI.fp (12446–12472, 5′-CCTAATCTCAGCCATGGATCTCGC-TGC-3′) and 617a.ncoI.rp (NcoI:13421–13401, 5′-TTACCATGGAA-ATATCAAAGTTCTCCATCTG-3′)] was cloned inside in the sense orientation, giving rise to p617–71. Sequencing showed the *AGM* coding region to contain no base pair errors. This AGMpromoter::*AGM*::*GUS* reporter construct was then cloned as a *Xba*I, *Sal*I fragment into *Xba*I, *Xho*I-digested pBHS to give rise to p617–92. p617–92 was electroporated into GV3101 and transformed into wild-type Col-0 plants using the floral dip method. The *AGM*-like promoter was amplified by PCR from the BAC clone IGF_B122K2419, using primers 48.2.fp (XhoI:23577–23607, 5′-ATACTCGAGCAAGACAACGATCCAATAA-TCATTTGATCTCTC-3′) and 48.2.fr.rp (24577–24546, 5′-AAGATC-CATGGCGGATTTAGATATCAAGATC-3′) and cloned into pGEMTeasy to create p617–2. The AGM-like promoter from p617–2 was subsequently cloned as a *Xho*I-blunt, *Nco*I fragment upstream of the *uidA* gene, by cloning into *Sma*I/*Nco*I digested pblu-KS35SGUS to create p617–34. p617–34 was then sub-cloned as a *Sac*I/*Sal*I fragment into *Sac*I/*Xho*I-digested pBHS to create p617–38, suitable for electroporation into GV3101 for use in plant transformation. The AGM-like promoter contained no PCR-induced errors as deduced by sequencing.

Over-expression constructs

The *AGM* coding region was obtained as an *Nco*I, *Hin*dIII fragment from the p617–11 plasmid (see Complementation procedures) This 1,313-bp fragment was blunted and cloned into the *Sma*I-digested pB35SXS binary vector, downstream of the CamV35S promoter. pB35SXS is based on the pBHS vector, containing the full-length 35S cauliflower mosaic virus promoter inserted as a *Hin*dIII, *Xba*I fragment. PCR was utilized to identify clone p617–51, containing the *AGM* gene in the sense orientation. P617–51 was electroporated into *Agrobacterium* strain, GV3101 and introduced into a Col-0 background by floral dipping.

The *AGM*-like promoter and coding region was obtained by PCR using the EXPAND system (as described above) using primers 48.2.fp (see GUS results above) and 48.2.rp (XbaI, 25533–25506: 5′-TATTC-TAGATCAAACTTCAAAGTTCTCCATTTGAATG-3′) and sub-cloned into pGEMTeasy creating p617–1. Sequencing of p617–1 showed 3 bp errors in the coding region at positions 24849 (T to G transition) 25388 (A to G transition) and 25188 (C to T transition). Subsequently, only the *AGM*-like coding region was excised from 617–1 as an *Nco*I, *Xba*I fragment and blunted, allowing cloning into *Sma*I-digested pB35SXS resulting in p617–52. p617–52 was electroporated into GV3101 and introduced into a Col-0 background by floral dipping.

Selection of transgenic plant lines, GUS analysis, sectioning and sequence analysis

These methods were carried out as described previously (Sorensen et al. 2003). Additionally, following GUS staining and Araldite embedding 0.5 μm sections were counterstained with 0.1% safranin.

Acknowledgments

Grateful thanks to Martina Kania for greenhouse assistance. This project was jointly funded by the German federal ministry BMBF in the context of the plant genomics program ZIGIA (Foerderkennzeichen 0311751) as well as the following German plant breeding companies: Aventis Crop Sciences, Deutsche Saatveredelung, KWS Saat AG and Nord-deutsche Pflanzenzucht.

References

Christensen, C.A., Gorsich, S.W., Brown, R.H., Jones, L.G., Brown, J., Shaw, J.M. and Drews, G.N. (2002) Mitochondrial GFA2 is required for synergid cell death in Arabidopsis. *Plant Cell* 14: 2215–2232.

Christensen, C.A., King, E.J., Jordan, J.R. and Drews, G.N. (1997) Megagametogenesis in Arabidopsis wild-type and the Gf mutant. *Sexual Plant Reprod.* 10: 49–64.

Christensen, C.A., Subramanian, S. and Drews, G.N. (1998) Identification of gametophytic mutations affecting female gametophyte development in Arabidopsis. *Dev. Biol.* 202: 136–151.

Drews, G.N., Lee, D. and Christensen, C.A. (1998) Genetic analysis of female gametophyte development and function. *Plant Cell* 10: 5–18.

Feldmann, K.A., Coury, D.A. and Christianson, M.L. (1997) Exceptional segregation of a selectable marker (Kan(R)) in Arabidopsis identifies genes important for gametophytic growth and development. *Genetics* 147: 1411–1422.

Goldberg, R.B., Beals, T.P. and Sanders, P.M. (1993) Anther development: basic principles and practical applications. *Plant Cell* 5: 1217–1229.

Grini, P.E., Jurgens, G. and Hulskamp, M. (2002) Embryo and endosperm development is disrupted in the female gametophytic capulet mutants of Arabidopsis. *Genetics* 162: 1911–1925.

Holding, D.R. and Springer, P.S. (2002) The Arabidopsis gene PROLIFERA is required for proper cytokinesis during seed development. *Planta* 214: 373–382.

Howden, R., Park, S.K., Moore, J.M., Orme, J., Grossniklaus, U. and Twell, D. (1998) Selection of T-DNA-tagged male and female gametophytic mutants by segregation distortion in Arabidopsis. *Genetics* 149: 621–631

Li, Y., Rosso, M.G., Strizhov, N., Viehoever, P. and Weisshaar, B. (2003) GABI-Kat SimpleSearch: a flanking sequence tag (FST) database for the identification of T-DNA insertion mutants in *Arabidopsis thaliana*. *Bioinformatics* 19: 1441–1442.

Moore, J.M., Calzada, J.P.V., Gagliano, W. and Grossniklaus, U. (1997) Genetic characterization of hadad, a mutant disrupting female gametogenesis in *Arabidopsis thaliana*. *Cold Spring Harbor Symp. Quant. Biol.* 62: 35–47.

Schneitz, K., Hulskamp, M. and Pruitt, R.E. (1995) Wild-type ovule development in *Arabidopsis thaliana* – a light-microscope study of cleared whole-mount tissue. *Plant J.* 7: 731–749.

Scott, R., Hodge, R., Paul, W. and Draper, J. (1991) The molecular biology of anther differentiation. *Plant Sci.* 80: 167–191.

Sorensen, M.B., Chaudhury, A.M., Robert, H., Bancharel, E. and Berger, F. (2001) Polycomb group genes control pattern formation in plant seed. *Curr. Biol.* 11: 277–281.

Sorensen, A.M., Krober, S., Unte, U.S., Huijser, P., Dekker, K. and Saedler, H. (2003) The Arabidopsis ABORTED MICROSPORES (AMS) gene encodes a MYC class transcription factor. *Plant J.* 33: 413–423.

Springer, P.S., Holding, D.R., Groover, A., Yordan, C. and Martienssen, R.A. (2000) The essential Mcm7 protein PROLIFERA is localized to the nucleus of dividing cells during the G(1) phase and is required maternally for early Arabidopsis development. *Development* 127: 1815–1822.

Springer, P.S., McCombie, W.R., Sundaresan, V. and Martienssen, R.A. (1995) Gene trap tagging of Prolifera, an essential Mcm2-3-5-like gene in Arabidopsis. *Science* 268: 877–880.

Steiner-Lange, S., Gremse, M., Kuckenberg, M., Nissing, E., Schächtele, D., Spenrath, N., Wolff, M., Saedler, H. and Dekker, K. (2001) Efficient identification of Arabidopsis knock-out mutants using DNA-arrays of transposon flanking sequences. *Plant Biol.* 3: 391–397.

Twell, D., Park, S.K. and Lalanne, E. (1998) Asymmetric division and cell-fate determination in developing pollen. *Trends Plant Sci.* 3: 305–310.

Webb, M.C. and Gunning, B.E.S. (1994) Embryo sac development in *Arabidopsis thaliana*. 2. The cytoskeleton during megagametogenesis. *Sexual Plant Reprod.* 7: 153–163.

(Received September 4, 2003; Accepted April 26, 2004)